NANO LETTERS

pubs.acs.org/NanoLett

Letter

Nanozyme-Enhanced Probiotic Spores Regulate the Intestinal Microenvironment for Targeted Acute Gastroenteritis Therapy

Gen Wei, Wanling Liu, Yihong Zhang, Zijun Zhou, Yuting Wang, Xiaoyu Wang, Shuaishuai Zhu, Tong Li, and Hui Wei*

Cite This: *Nano Lett.* 2024, 24, 2289−2298

Read Online

ACCESS | Metrics & More | Article Recommendations | Supporting Information

ABSTRACT: Antibiotic therapeutics to combat intestinal pathogen infections often exacerbate microbiota dysbiosis and impair mucosal barrier functions. Probiotics are promising strategies, because they inhibit pathogen colonization and improve intestinal microbiota imbalance. Nevertheless, their limited targeting ability and susceptibility to oxidative stress have hindered their therapeutic potential. To tackle these challenges, Ces_3 is synthesized by *in situ* growth of CeO_2 nanozymes with positive charges on probiotic spores, facilitating electrostatic interactions with negatively charged pathogens and possessing a high reactive oxygen species (ROS) scavenging activity. Importantly, Ces_3 can resist the harsh environment of the gastrointestinal tract. In mice with *S.* Typhimurium-infected acute gastroenteritis, Ces_3 shows potent anti-*S.* Typhimurium activity, thereby alleviating the dissemination of *S.* Typhimurium into other organs. Additionally, owing to its O_2 deprivation capacity, Ces_3 promotes the proliferation of anaerobic probiotics, reshaping a healthy intestinal microbiota. This work demonstrates the promise of combining antibacterial, anti-inflammatory, and O_2 content regulation properties for acute gastroenteritis therapy.

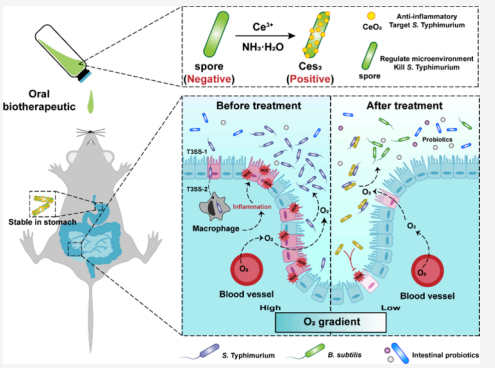

KEYWORDS: *nanozymes, probiotics, acute gastroenteritis therapy, microbiota, intestinal microenvironment*

Acute gastroenteritis, a common inflammatory intestinal disease, is usually caused by food-borne *Salmonellae*, such as *Salmonella enterica* serovar Typhimurium (*S.* Typhimurium).[1,2] The intestinal microenvironment, which plays a key role in maintaining healthy intestinal microbiota, is altered during *S.* Typhimurium infection.[3,4] Specifically, *S.* Typhimurium uses type III secretion system-1 (T3SS-1) and T3SS-2 to invade the intestinal epithelium and survive in the tissue of the host, respectively. Both of these processes trigger the acute intestinal inflammation by boosting reactive oxygen species (ROS) levels and increasing oxygen (O_2) content.[5,6] On the one hand, elevated ROS can promote *S.* Typhimurium expansion through nitrate respiration; on the other hand, because nearly all beneficial bacteria are obligate anaerobes, exposure to O_2 can induce toxicity to them.[6,7] These changes in the inflammatory intestinal microenvironment eventually damage mucosal barrier functions and lead to intestinal microbiota imbalance.[8,9]

The first-line antibiotics used in the treatment of salmonellosis, such as fluoroquinolones, possess broad-spectrum antibacterial properties. Prolonged usage of these antibiotics leads to the enrichment of resistant strains, potentially giving rise to superbugs, which can aggravate the imbalance in intestinal microbiota and impair the mucosa.[9−11] Moreover, antibiotics have a minimal effect on the elevated level of the O_2 level. In contrast, probiotics generate beneficial and active metabolites, which inhibit the growth of pathogens and facilitate the proliferation of other probiotics. This mechanism helps maintain the delicate balance of intestinal microbiota.[12,13] Among probiotics, the dormant spores formed by *Bacillus subtilis* (*B. subtilis*) have received increasing attention because they can resist harsh gastrointestinal (GI) environmental assaults. Furthermore, its germination to probiotic *B. subtilis*, accompanied by O_2 consumption, can enhance the beneficial bacteria and consequently improve the intestinal microenvironment.[14−16] Nevertheless, the therapeutic efficacy of spores on acute gastroenteritis is not satisfactory due to a couple of limitations. First, spores exhibit negligible ROS scavenging activity, which hinders mucosal repair. Second, there is a lack of control over the location of spore germination in the intestinal tract, resulting in insufficient viable *B. subtilis* in the vicinity of *S.* Typhimurium.[5,17,18] Therefore, we reason that improving the ROS-scavenging activity and *S.* Typhimurium-targeting capacity of spores would be a promising strategy to enhance their therapeutic efficacy.

Received: November 24, 2023
Revised: February 6, 2024
Accepted: February 7, 2024
Published: February 11, 2024

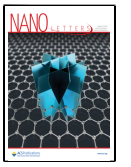

https://doi.org/10.1021/acs.nanolett.3c04548
Nano Lett. 2024, 24, 2289−2298

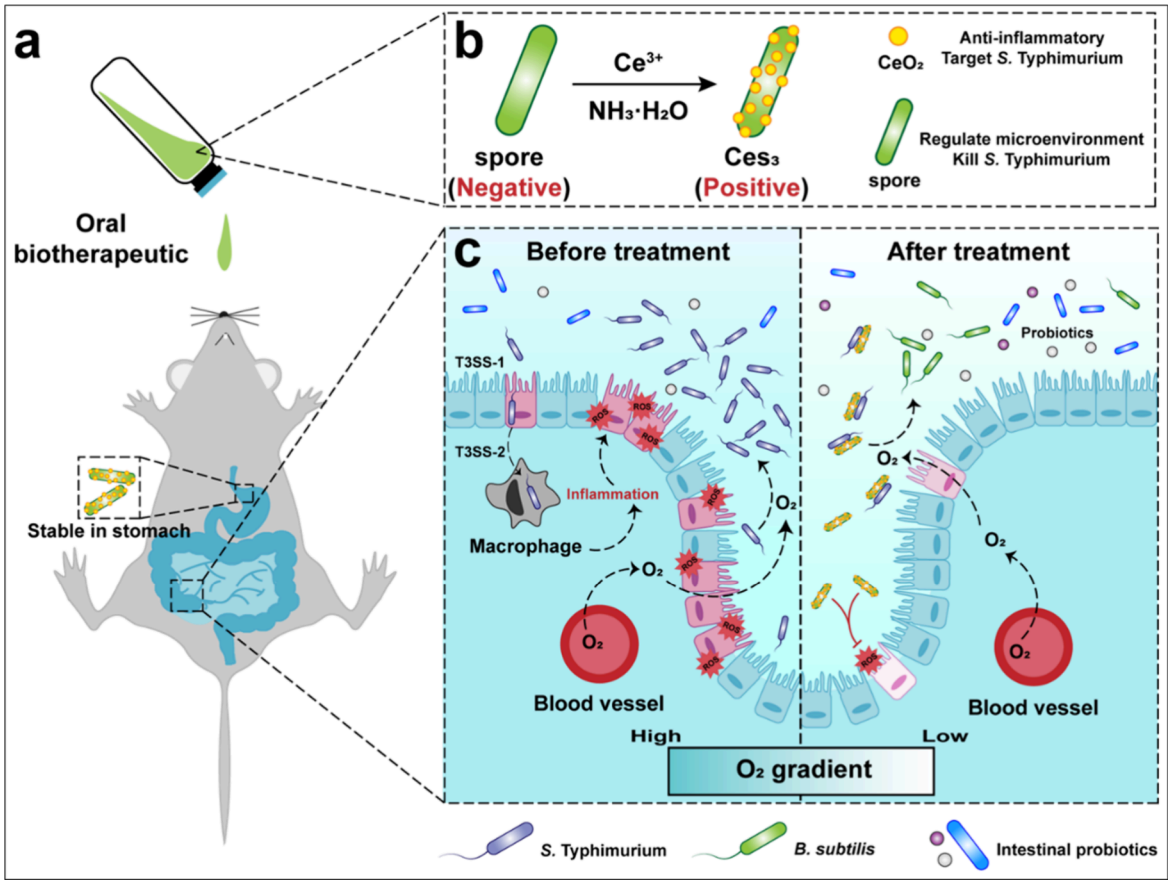

Figure 1. (a) Ces_3-mediated protective effects against GI environmental assaults as an oral biotherapeutic. (b) Preparation of Ces_3 by *in situ* growth of CeO_2 nanozymes (positively charged) on spores (negatively charged). (c) Left: Acute gastroenteritis microenvironment characterized by elevated intestinal epithelial ROS levels and O_2 content, damaged intestinal mucosal cells, and imbalance of intestinal microbiota (hyperproliferating *S.* Typhimurium and extremely reduced anaerobic probiotics). Right: Ces_3 promotes cures in acute gastroenteritis, through targeting *S.* Typhimurium and persistent antioxidant activity as well as rapid O_2 deprivation, eradicating *S.* Typhimurium and ameliorating the intestinal microbiome.

Recently, ROS scavenging nanozymes have garnered significant attention due to their advantages over natural enzymes and conventional enzyme mimics.[19−25] Among them, cerium oxide (CeO_2) nanozymes are particularly promising for biomedical applications because of their stability in acidic biofluids, positively charged characteristics, and potent ROS scavenging activity.[26−29] Accordingly, the use of CeO_2 nanozymes would tackle the limitations of spores by imparting them with ROS-scavenging activity and *S.* Typhimurium-targeting capacity through electrostatic interactions.

Herein, CeO_2 nanozyme decorated spores (CeO_2/spores) were fabricated by *in situ* growth of CeO_2 nanozymes on probiotic spores to effectively treat *S.* Typhimurium-induced acute gastroenteritis. After oral administration, the optimized CeO_2/spores, Ces_3 (Ces_3 represents a 3:1 mass ratio of spores to $Ce(NO_3)_3{\cdot}6H_2O$), could resist GI environmental assaults and then targeted *S.* Typhimurium (negatively charged) (Figure 1a,b). Subsequently, O_2 facilitated the germination of spores to form planktonic *B. subtilis* at the action site, effectively killing *S.* Typhimurium and regulating the intestinal microenvironment. Concurrently, CeO_2 nanozymes could reduce mucosal damage by scavenging ROS, which further promoted the balance of the intestinal microbiota. Importantly, *in vivo* therapeutic studies substantiate that Ces_3 was much friendlier than levofloxacin (a common oral antibiotics) to the intestinal anaerobic probiotic microbes and epithelial barrier, reshaping a healthier intestine (Figure 1c). This research provides a representative paradigm of nanozymes for pathogen-targeting acute gastroenteritis therapy by simultaneously regulating the intestinal microenvironment and eradicating *S.* Typhimurium.

To minimize the effects of high temperature and prolonged reaction times on probiotic spore germination,[15,30] we selected nanozymes that could be prepared in a short time at room temperature through a one-step reduction. As shown in Figures S1−S3, three nanozyme-decorated spores (X/spores) (X = CeO_2, Cu_2O, and Rh) were successfully synthesized by using a rapid and facile method with spores as templates.[26,31,32] Furthermore, we examined the superoxide dismutase (SOD)-like activity of X/spores. As shown in Figure S4a, both CeO_2/spores and Rh/spores had excellent SOD-like activities in comparison to Cu_2O/spores. While CeO_2/spores demonstrated good biocompatibility, Rh/spores exhibited cytotoxicity (Figure S4b). Additionally, to effectively target pathogens via electrostatic interactions, it was essential for X/spores to possess positive charges. We measured the zeta potentials of spores, pathogens, and X/spores. Figure S4c showed that only CeO_2/spores could reverse the negative charge of spores. Combined with excellent SOD-like activity, biocompatibility, and positive charges (Figure S4d), CeO_2/spores were selected for further investigation after our comprehensive evaluation.

https://doi.org/10.1021/acs.nanolett.3c04548
Nano Lett. 2024, 24, 2289−2298

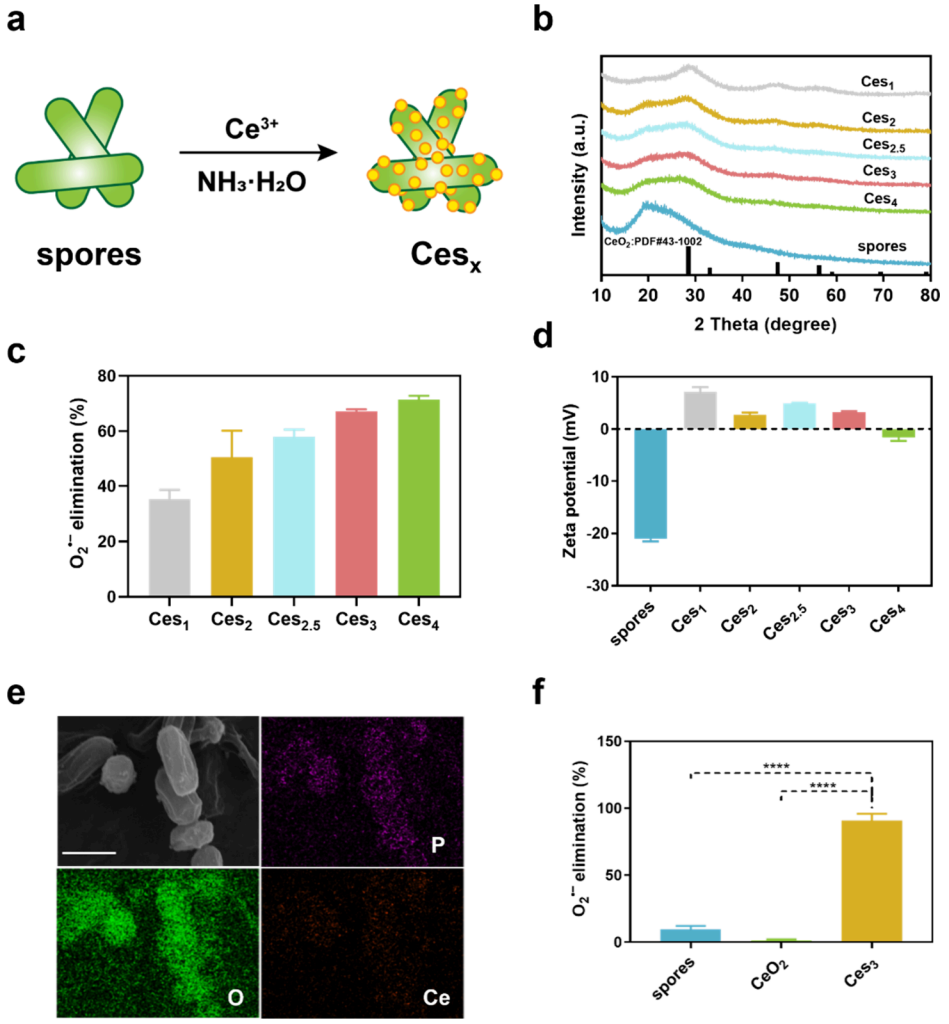

Figure 2. Synthesis and characterization of Ces_x. (a) Schematic representation of the preparation of Ces_x. (b) XRD patterns of spores and Ces_x. The lines at the bottom mark the reference patterns of CeO_2 (JCPDS Card No. 43-1002). a.u., arbitrary units. (c) SOD-like activity and (d) zeta potentials of Ces_x. (e) Element mapping (P, O, and Ce) of Ces_3. Scale bar: 1 μm. (f) SOD-like activities of spores, CeO_2, and Ces_3. Data are presented as means ± SD (n = 3).

To further optimize the formulation, different concentrations of $Ce(NO_3)_3{\cdot}6H_2O$ were used to synthesize CeO_2/spores. The corresponding products were denoted as Ces_x (where x = 1, 2, 2.5, 3, and 4, representing different ratios of spores to $Ce(NO_3)_3{\cdot}6H_2O$) (Figure 2a). The XRD patterns displayed that Ces_1, Ces_2, $Ces_{2.5}$, Ces_3, and Ces_4 had similar characteristic peaks indexed to the spores and CeO_2 (Figure 2b). Then, their SOD-like activities were evaluated. The Ces_x samples, normalized to a CeO_2 nanozyme content of 20 μg/mL, showed a trend of Ces_4 > Ces_3 > $Ces_{2.5}$ > Ces_2 > Ces_1 (Figure 2c). The trend of SOD-like behavior was attributed to the improved dispersibility of CeO_2 nanozymes on the spore surface, as confirmed by SEM imaging (Figure S5). Notably, all Ces_x, except Ces_4, exhibited positive zeta potentials (Figure 2d). The above results indicated that Ces_3, possessing both high SOD-like activity and positive charges, is promising for subsequent studies. As visualized in Figure 2e and Figure S6, the SEM elemental mapping images verified the presence of C, N, O, P, S, and Ce elements in Ces_3. Specifically, Ce and O were uniformly distributed on the surface of spores. Furthermore, Ces_3 (the concentration of Ce on Ces_3 by inductively coupled plasma (ICP) was 16.28 μg/mL (Table S1)) exhibited enhanced SOD-like activity compared with CeO_2 nanozymes or spores alone (Figure 2f). In general, pristine CeO_2 nanozymes aggregated seriously and their average size was much higher than that of CeO_2 on spores (Figure S7a,b). While CeO_2 on spores aggregated slightly (the red circle) (Figure S7b), CeO_2 could be well stabilized and dispersed on spores, ensuring catalytic performance.

During the nanozyme synthesis process, we added different concentrations of Ce^{3+}, $NH_3{\cdot}H_2O$ (8%, w/v), and EG (50%, w/v), respectively. The Ce^{3+} contents of Ces_1, Ces_2, $Ces_{2.5}$, Ces_3, and Ces_4 were 11.51 mM, 9.21 mM, 6.91 mM, 4.61 mM, and 2.30 mM. As shown in Figure 3a and Figures S8−S11, the viability of the spores was retained both before and after the nanozyme preparation process, which is critical for spore germination to *B. subtilis* and retaining antibacterial activity. The rationale behind using *B. subtilis* cell-free supernatants to test antibacterial activity is rooted in the secretion of lipopeptides by planktonic *B. subtilis*. The lipopeptides include surfactins, iturins, fengycins, *etc.*, which are the key components to elicit antibacterial activity. On the one hand, these lipopeptides are amphiphilic that effectively dissolve in LB medium;[14,16,33] on the other hand, to minimize the interference of *B. subtilis* on the OD value (600 nm), we used *B. subtilis* cell-free supernatants from Ces_3 germination at

https://doi.org/10.1021/acs.nanolett.3c04548
Nano Lett. 2024, 24, 2289−2298

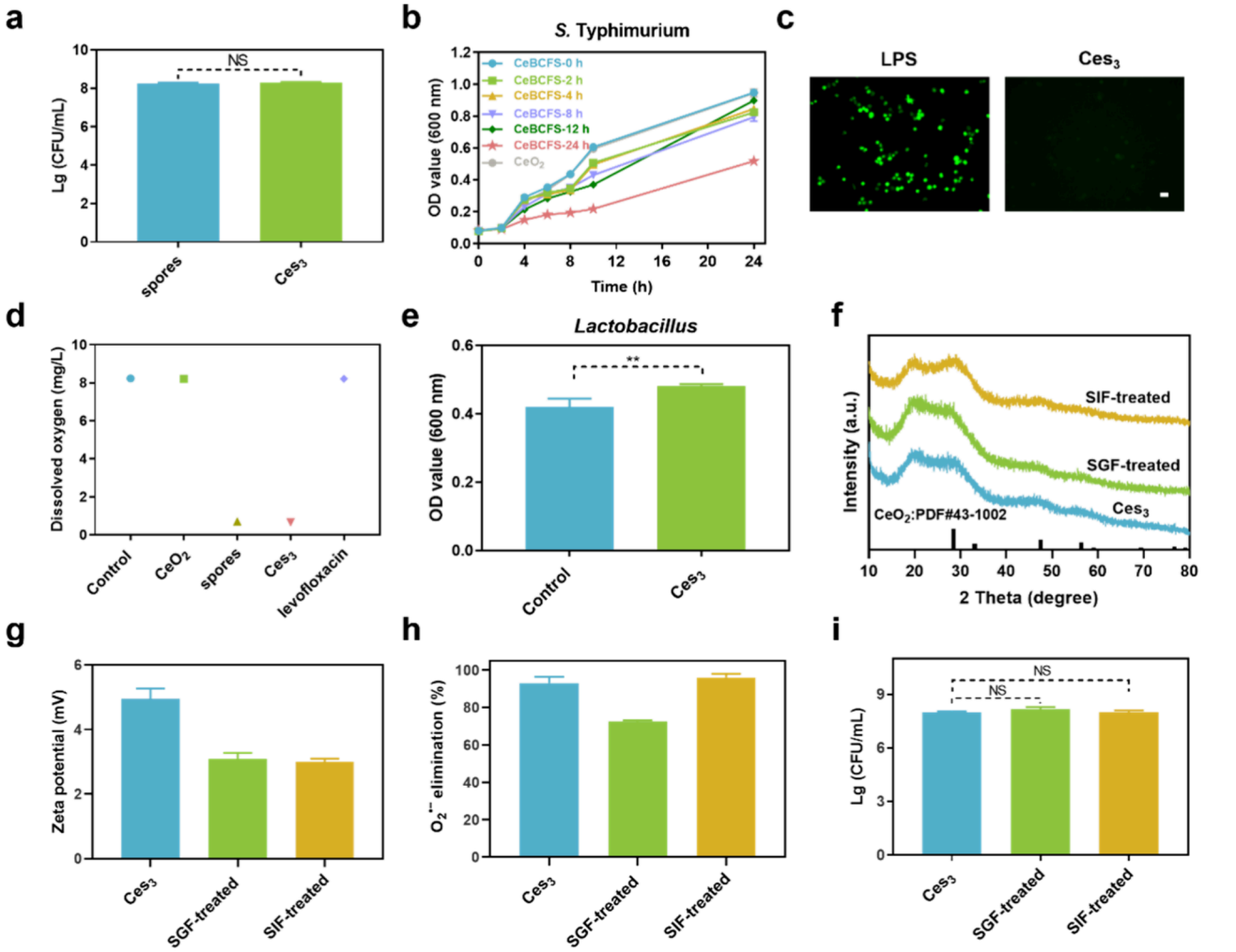

Figure 3. Antibacterial, anti-inflammatory, and O_2 deprivation activities of Ces_3 *in vitro*. (a) Effects of Ces_3 on the viability of spores. (b) Anti-*S.* Typhimurium activities of supernatants from Ces_3 fermentation for different times (0, 2, 4, 8, 12, and 24 h). Samples were taken out for OD_{600nm} evaluation at indicated incubation time points. (c) Fluorescence microscopy images of ROS levels in RAW264.7 cells treated in the Ces_3 group followed by LPS. Scale bar, 20 μm. (d) Dissolved oxygen consumption tests of indicated groups in the liquid LB medium. (e) Effects of Ces_3 on the viability of *Lactobacillus* in a microaerobic environment. *Lactobacillus* samples were taken out for OD_{600nm} evaluation at 24 h. (f) XRD patterns of Ces_3 treated with SGF or SIF. The lines at the bottom mark the reference patterns of CeO_2 (JCPDS Card No. 43-1002). Zeta potentials (g), SOD-like activities (h), and survivals (i) of spores in Ces_3 followed by SGF or SIF treatment. The concentrations of CeO_2, spores, Ces_3, and levofloxacin were 20, 380, 400, and 200 μg/mL, respectively. Data are presented as means ± SD (n = 3).

different times (designated as CeBCFS-0, 2, 4, 8, 12, and 24 h) against both Gram-negative and Gram-positive bacteria. The germination supernatants for spores at the same times (i.e., BCFS-0, 2, 4, 8, 12, and 24 h) and CeO_2 nanozymes were used for comparison. We showed that CeBCFS-24 h and BCFS-24 h treatments consistently exhibited the lowest OD_{600nm} values for both Gram-negative and Gram-positive bacteria, whereas CeO_2 nanozymes treatment exhibited very high OD_{600nm} values. These results implied that Ces_3 had excellent antibacterial ability similar to that of spores, while CeO_2 nanozymes had negligible antibacterial activity (Figure S12, Figure 3b, and Figure S13a-c). Consequently, CeBCFS-24 h was selected, and a treatment duration of 24 h was optimal for further analysis.

To assess the antibacterial mechanism of CeBCFS-24 h, we next investigated the effects of pH changes on bacterial growth. As shown in Figures S14 and S15, while CeBCFS-24 h increased the pH of the LB medium from 6.8 to 8.0, this pH change had negligible effects on bacterial proliferation. These results verified that Ces_3 germination-induced pH changes were not responsible for the antibacterial effects. Afterward, we analyzed the structural integrity and morphology of *S.* Typhimurium treated with CeBCFS-24 h. The confocal fluorescence images depicted that CeBCFS-24 h severely damaged the membrane of *S.* Typhimurium, as evidenced by the presence of membrane-impermeable propidium iodide (PI) molecules (Figure S16).[34] Further morphological observation by SEM imaging verified large amounts of ruptured bacterial cells (Figure S17). In addition, we evaluated the effects of CeBCFS-24 h on genomic DNA and whole-cell and membrane proteins of *S.* Typhimurium.[33,35] As visualized in Figure S18, compared with the control, the CeBCFS-24 h-treated group induced partial DNA degradation, leading to alterations in whole-cell proteins.

As designed, the CeO_2-coated spores were positively charged, therefore preferentially targeting negatively charged *S.* Typhimurium through electrostatic interactions. Such a design ensured sufficient viable spores in the vicinity of *S.* Typhimurium exert antibacterial effects. To verify this

https://doi.org/10.1021/acs.nanolett.3c04548
Nano Lett. 2024, 24, 2289−2298

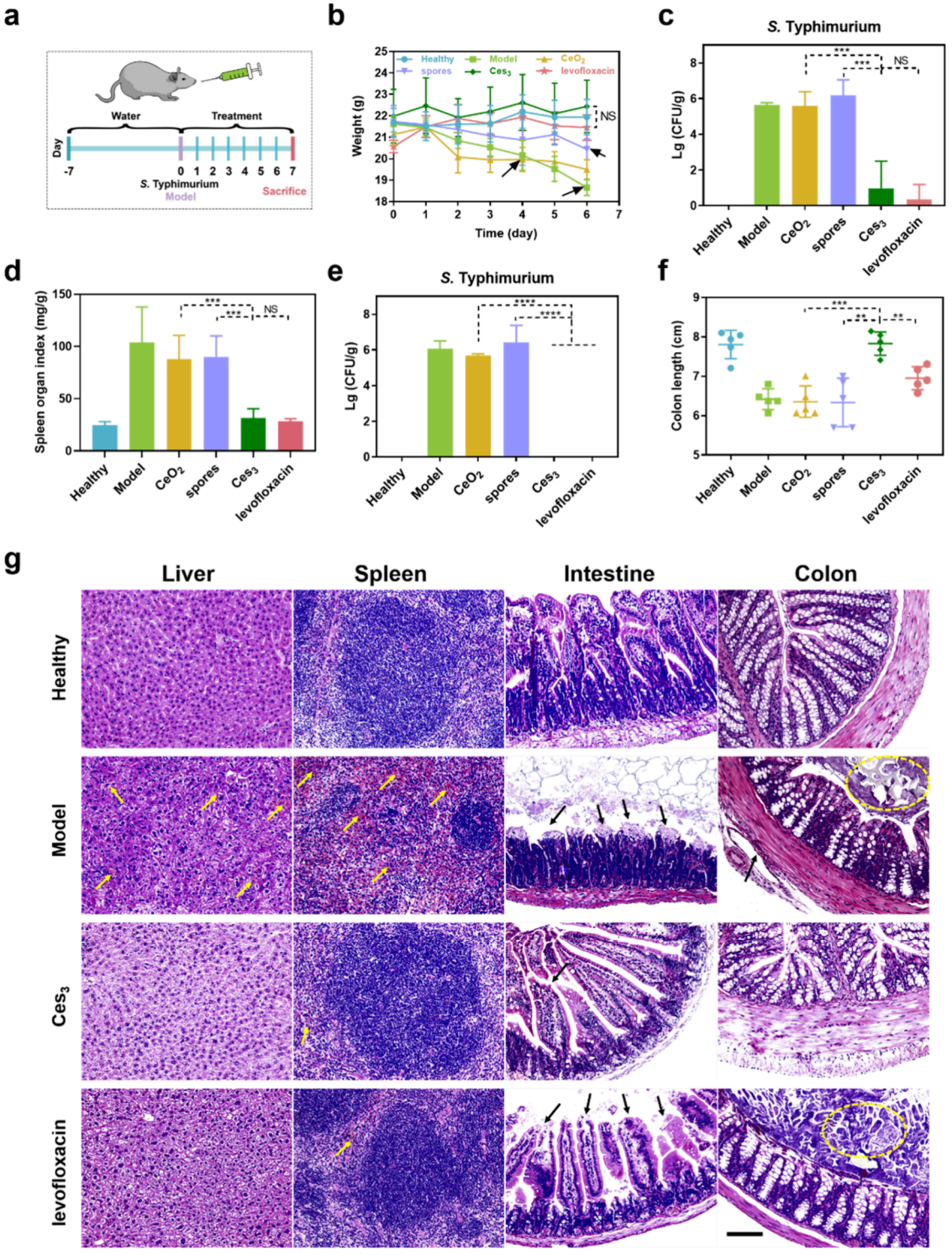

Figure 4. Therapeutic efficacy of Ces_3 on *S.* Typhimurium-induced acute gastroenteritis *in vivo*. (a) Experimental design and treatment protocols of the *S.* Typhimurium-infected mouse model of acute gastroenteritis. (b) Daily body-weight development for 7 days. Black arrows indicate that one mouse has died in the group. (c) *S.* Typhimurium counts in the gastrointestinal tracts. Spleen organ index (d) and corresponding CFU per gram (CFU/g) of *S.* Typhimurium (e). (f) Quantification of colon length in the indicated groups. (g) Representative H&E-staining images of the liver, spleen, intestine, and colon tissues in Healthy, Model, Ces_3, and levofloxacin groups. Scale bar: 100 μm. Yellow arrows and red circles indicate the location of tissue damage. The concentrations of CeO_2, spores, Ces_3, and levofloxacin were 1, 19, 20, and 13 mg/kg, respectively. Data are presented as means ± SD (n = 5).

hypothesis, we first analyzed the targeting properties of Ces_3 onto *S.* Typhimurium-coated (negatively charged, mimicking the infection site) polystyrene surfaces at 37 °C for 3 h *in vitro*. As shown in Figure S19a, compared with the spore group, *S.* Typhimurium-coated polystyrene surfaces treated with Ces_3 had higher amounts of spores. The preferential targeting of Ces_3 to *S.* Typhimurium-coated plates was attributed to the electrostatic interaction between them (Figure S19b).

https://doi.org/10.1021/acs.nanolett.3c04548
Nano Lett. 2024, 24, 2289−2298

Studies suggest that *S.* Typhimurium can trigger the acute intestinal inflammation and boost ROS levels.[5] The excess ROS and sustained oxidative stress can initiate an inflammatory cycle and amplify oxidative stress.[36] To stimulate the overproduction of intracellular ROS levels, lipopolysaccharide (LPS), an endotoxin extracted from the outer membrane of Gram-negative bacteria, was applied to treat the cells. The intracellular ROS levels were detected using 2′,7′-dichlorodihydrofluorescein diacetate (DCFH-DA) as a fluorescence probe. As displayed in Figure 3c and Figure S20a, the Ces_3-treated group showed the lowest fluorescence compared to CeO_2 and spores treatments, demonstrating the excellent ROS scavenging ability of Ces_3. These results were also confirmed through quantitative analysis of intracellular ROS using flow cytometry (Figure S20b).

In addition to elevated ROS levels, the abnormal intestinal microenvironment caused by *S.* Typhimurium is characterized by an increased epithelial O_2 content. In consideration of the obligate aerobic peculiarity of *B. subtilis*, the environmental oxygen is expected to be massively consumed, which in turn promotes proliferation of other probiotics.[3,7,37] As shown in Figure 3d, Ces_3 sprouted and tremendously exhausted dissolved O_2 in liquid LB medium within 24 h, similar to the effect observed with spores. In contrast, levofloxacin had a negligible effect on the O_2 content. To further demonstrate the critical role of environmental oxygen in probiotic proliferation, the probiotic *Lactobacillus* (yogurt source) was employed as an example to grow in aerobic, microaerobic, and anaerobic microenvironments (O_2 concentrations were 20%, 8%, and 0%, respectively). The results revealed that the anaerobic conditions were most conducive to *Lactobacillus* growth (Figure S21). Under the microaerobic microenvironment, which mimicked the O_2 levels of *S.* Typhimurium infection,[3] Ces_3 significantly promoted the proliferation of *Lactobacillus* (Figure 3e). Collectively, Ces_3 would be a promising candidate for *S.* Typhimurium-infected acute gastroenteritis therapy due to its antibacterial (by preferentially targeting *S.* Typhimurium), anti-inflammatory, and intestinal microenvironment amelioration behaviors.

Oral probiotics often encounter the challenge of GI environmental assaults.[38] It is critical that Ces_3 be stable in the stomach and small intestine to ensure higher bioavailability. We examined morphological changes in Ces_3 by using SEM imaging after exposure to simulated gastric fluid (SGF) and simulated intestinal fluid (SIF). As shown in Figure S22a,b, after incubation in SGF or SIF for 4 h, Ces_3 retained its original morphology, consistent with the morphology in Figure 2e and Figure S5e. Then, we studied the crystalline structures of Ces_3. The XRD patterns showed that Ces_3 treated with SGF or SIF retained its crystalline structure (Figure 3f), akin to that of untreated Ces_3 (Figure 2b). We also assessed the zeta potentials, SOD-like activities, and viability of Ces_3. As shown in Figure 3g–i and Figures S23 and S24, after a 4 h exposure to SGF or SIF, Ces_3 retained the positive charges, high ROS scavenging activity, and comparable spore viability to that of spores alone. These results suggested that Ces_3 as an oral medication has great potential for treating acute gastroenteritis caused by *S.* Typhimurium as it effectively resists the environmental assaults encountered in the GI tract.

Before the therapeutic study, the cell viability of RAW264.7 cell lines treated by CeO_2 nanozymes, spores, and Ces_3 was evaluated. The results revealed that CeO_2, spores, and Ces_3 at 20, 380, and 400 μg/mL exhibited no obvious cytotoxicity (Figure S25). Importantly, both spores at 380 μg/mL and Ces_3 at 400 μg/mL produced around 10^8 CFU/mL alive *B. subtilis* (Figure S26), which meets the requirements for oral delivery of probiotics.[39] On the basis of the results of biocompatibility and CFU measurement, CeO_2, spores, and Ces_3 at 20, 380, and 400 μg/mL were optimal for the subsequent animal experiments. An overview of the experimental procedure is presented in Figure 4a. C57BL/6 mice were injected (intragastric administration) with *S.* Typhimurium solutions by gavage to induce acute gastroenteritis. Subsequently, sterile phosphate buffered saline (PBS; Model), CeO_2 nanozymes, spores, Ces_3, and levofloxacin (a representative medication for acute gastroenteritis therapy, was included for comparison) were orally administered for seven consecutive days (day 0 to day 6), and the therapeutic efficacy was evaluated on day 7 after euthanasia and dissection of mice.

Compared with other groups, Ces_3 and levofloxacin treatments prevented weight loss, death (indicated by the black arrows), and fur scruffiness caused by *S.* Typhimurium infection (Figure 4b and Figure S27). Additionally, *S.* Typhimurium in the gastrointestinal tract was quantified using the different colony morphologies of intestinal commensal bacteria (very small), fungi (very large), spores (very large), and *S.* Typhimurium (middle and transparent) on Sabouraud Dextrose Agar (SDA) medium (Figures S11 and S28). As shown in Figure 4c, because Ces_3 treatment obviously increased the number of spores in the gastrointestinal tracts (Figure S29), Ces_3 treatment obviously decreased the number of *S.* Typhimurium, similar to the levofloxacin group. Furthermore, given that the spleen and liver are susceptible to damage during acute gastroenteritis, we next investigated the changes in these two organs.[40] As depicted in Figure 4d and Figure S30, the organ index and size of the spleen in the Ces_3 and levofloxacin groups were significantly lower than those in other groups. Importantly, no *S.* Typhimurium was detected in the spleen and liver tissues (Figure 4e and Figure S31), indicating that Ces_3 had strong antibacterial activity, comparable to that of levofloxacin, thereby alleviating *S.* Typhimurium dissemination into the spleen and liver. In short, these results confirmed that the CeO_2 coating facilitated electrostatic interactions with negatively charged *S.* Typhimurium is used for improving delivery targeting of spores to exert antibacterial effects.

Notably, the colon length of Ces_3-treated mice was restored to normal, which was much longer than that of the levofloxacin-treated mice (Figure 4f and Figure S32). The result was attributed to the superior antioxidant properties of Ces_3 compared with levofloxacin.[26] In line with the above observations, hematoxylin and eosin (H&E) staining showed that the heart, lung, and kidney were not affected in all treatment groups (Figure S33). In contrast, severe tissue destruction and inflammatory infiltration were observed in the spleen, liver, intestine, and colon sections from untreated *S.* Typhimurium-infected mice. Note that the damage and inflammation in the intestine and colon were greatly alleviated after Ces_3 treatment, which was superior to that of levofloxacin (Figure 4g and Figure S34). In short, these findings suggested that although levofloxacin has strong anti-*S.* Typhimurium activity, Ces_3 notably reduces the risk of epithelial mucosa damage during acute gastroenteritis therapy.

The disturbance of the intestinal microbiome is closely related to acute gastroenteritis progression.[5,9] Encouraged by the promising therapeutic efficacy, we then evaluated whether

https://doi.org/10.1021/acs.nanolett.3c04548
Nano Lett. 2024, 24, 2289−2298

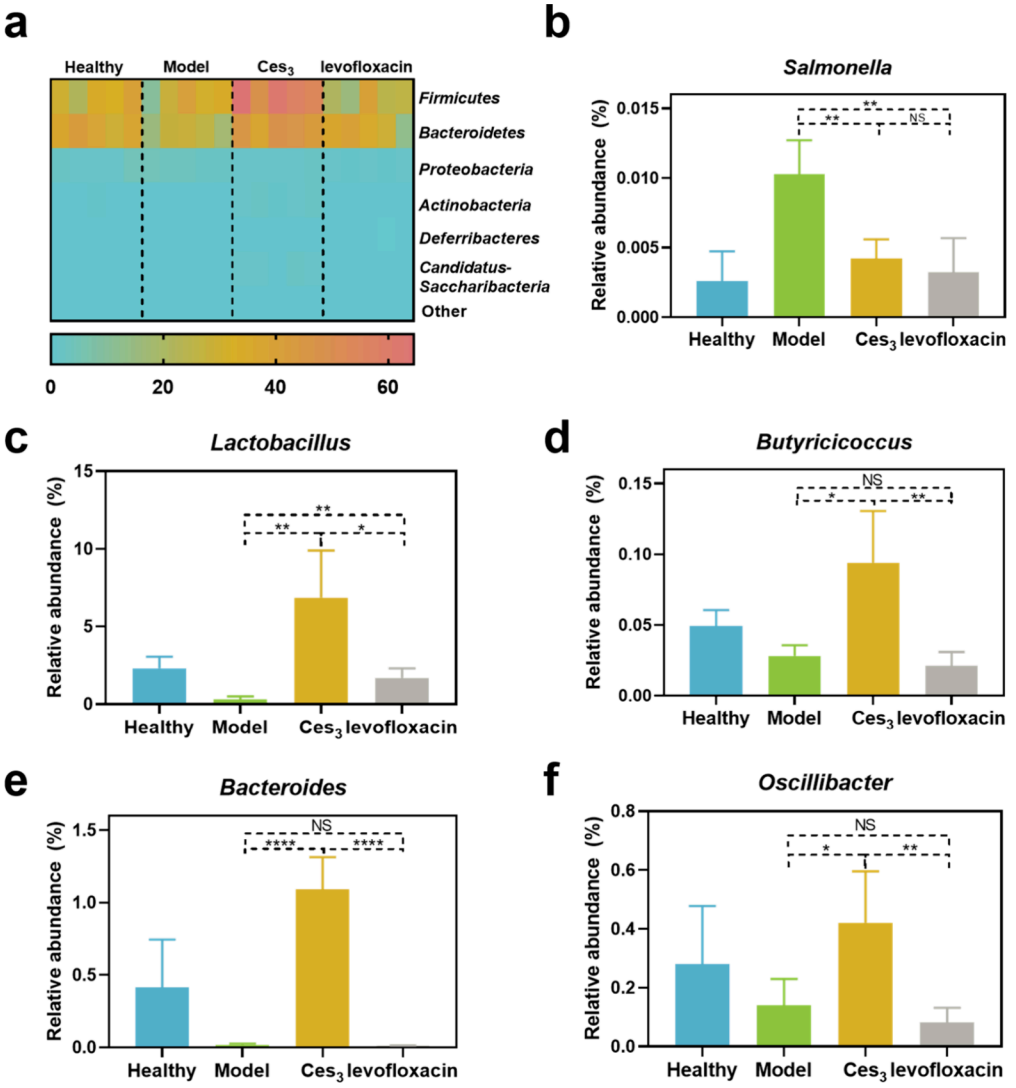

Figure 5. Ces_3, in comparison to levofloxacin, modulates intestinal microbiome homeostasis in the *S.* Typhimurium-induced mouse model of acute gastroenteritis. (a) Heat map illustrating the relative abundance of intestinal microbiome at the phylum level for each mouse (columns) after different treatments. Significant changes after Ces_3 treatment in the relative abundance of *Salmonella* (b), *Lactobacillus* (c), *Butyricicoccus* (d), *Bacteroides* (e), and *Oscillibacter* (f) at the genus level. The concentrations of Ces_3 and levofloxacin were 20 and 13 mg/kg, respectively. Data are presented as means ± SD (n = 5).

Ces_3 could better regulate the composition and abundance of the intestinal microbiome. As indicated by α-diversity (i.e., ACE and Chao1 indices), Ces_3 treatment improved bacterial diversity in mice with *S.* Typhimurium-infected acute gastroenteritis, reaching levels comparable to those of healthy mice. This improvement in diversity was superior to the results observed in the levofloxacin group (Figure S35a,b). A possible explanation is that levofloxacin, due to its broad-spectrum antibacterial properties, leads to a sharp decrease of intestinal probiotics.[11] Further analysis at the phylum/genus level uncovered that both Ces_3 and levofloxacin treatments obviously reduced the relative abundance of inflammatory disease-related *Proteobacteria* and subordinate classic pathogens such as *Salmonella* and *Escherichia-Shigella* (Figure 5a,b, Figure S36a, and Figure S37a). This suggested that Ces_3 had strong antipathogen behavior similar to levofloxacin, corroborating the results presented in Figure 4c.[41,42] Interestingly, compared to levofloxacin treatment, Ces_3 treatment increased the relative abundance of *Bacteroidetes*, which play pivotal roles in various metabolic activities beneficial to the host (Figure S36b).[43] In contrast, levofloxacin treatment increased the relative abundance of *Bilophila*, an opportunistic pathogen that thrives in inflamed samples (e.g., severe sepsis) (Figure S37b).[44,45] This shift altered the balance of the intestinal microbiome.

Importantly, owing to the O_2 deprivation activity of Ces_3, we further studied whether Ces_3 could promote the growth of anaerobic probiotics. As depicted in Figure 5c–f, compared to levofloxacin treatment, Ces_3 treatment increased the relative abundance of *Lactobacillus*, *Butyricicoccus*, *Bacteroides*, and *Oscillibacter*. These probiotics can promote the maintenance of intestinal homeostasis and inhibit pathogen translocation.[4,46,47]

In summary, Ces_3, possessing anti-*S.* Typhimurium, ROS-scavenging, and O_2 deprivation activities, was synthesized by *in situ* growth of CeO_2 nanozymes on spores. Ces_3 holds promise for targeted therapy in the treatment of acute gastroenteritis. Importantly, as an oral biotherapeutic, Ces_3 can resist GI environmental assaults. *In vivo* experiments confirmed its significant therapeutic efficacy. Ces_3 improved the intestinal microbiota, particularly by promoting the growth of anaerobic

https://doi.org/10.1021/acs.nanolett.3c04548
Nano Lett. 2024, 24, 2289−2298

probiotics, thus, reshaping a healthier intestinal microenvironment. This work not only demonstrates the advantages of nanozyme-enhanced probiotic spores over small molecular antibacterial drugs for the treatment of *S.* Typhimurium-infected acute gastroenteritis but also provides a promising strategy to design nanozyme-based oral biotherapeutics with simultaneous antibacterial, anti-inflammatory, and microenvironmental regulation properties for biomedical applications.

■ ASSOCIATED CONTENT

Supporting Information

The Supporting Information is available free of charge at https://pubs.acs.org/doi/10.1021/acs.nanolett.3c04548.

Materials and methods, including preparation and analysis of spores and Ces_x, SOD-like and antibacterial activity, live/dead cell staining and determination of DNA degradation of *S.* Typhimurium, *in vitro* cytotoxicity evaluation, detection of intracellular ROS-scavenging activity, dissolved oxygen deprivation behavior, the viability of spores after CeO_2 coating, targeting simulation and resistance assay of Ces_3 *in vitro*, animal protocols and statistical analysis along with additional references, and Figures S1−S37 and Tables S1−S3 (PDF)

■ AUTHOR INFORMATION

Corresponding Author

Hui Wei − *Department of Biomedical Engineering, College of Engineering and Applied Sciences, Nanjing National Laboratory of Microstructures, Jiangsu Key Laboratory of Artificial Functional Materials and State Key Laboratory of Analytical Chemistry for Life Science, School of Chemistry and Chemical Engineering, Chemistry and Biomedicine Innovation Center (ChemBIC), Nanjing University, Nanjing, Jiangsu 210023, China;* orcid.org/0000-0003-0870-7142; Email: weihui@nju.edu.cn

Authors

Gen Wei − *Department of Biomedical Engineering, College of Engineering and Applied Sciences, Nanjing National Laboratory of Microstructures, Jiangsu Key Laboratory of Artificial Functional Materials, Nanjing University, Nanjing, Jiangsu 210023, China*

Wanling Liu − *Department of Biomedical Engineering, College of Engineering and Applied Sciences, Nanjing National Laboratory of Microstructures, Jiangsu Key Laboratory of Artificial Functional Materials, Nanjing University, Nanjing, Jiangsu 210023, China*

Yihong Zhang − *Department of Biomedical Engineering, College of Engineering and Applied Sciences, Nanjing National Laboratory of Microstructures, Jiangsu Key Laboratory of Artificial Functional Materials, Nanjing University, Nanjing, Jiangsu 210023, China*

Zijun Zhou − *Department of Biomedical Engineering, College of Engineering and Applied Sciences, Nanjing National Laboratory of Microstructures, Jiangsu Key Laboratory of Artificial Functional Materials, Nanjing University, Nanjing, Jiangsu 210023, China*

Yuting Wang − *Department of Biomedical Engineering, College of Engineering and Applied Sciences, Nanjing National Laboratory of Microstructures, Jiangsu Key Laboratory of Artificial Functional Materials, Nanjing University, Nanjing, Jiangsu 210023, China*

Xiaoyu Wang − *Department of Biomedical Engineering, College of Engineering and Applied Sciences, Nanjing National Laboratory of Microstructures, Jiangsu Key Laboratory of Artificial Functional Materials, Nanjing University, Nanjing, Jiangsu 210023, China; Department of Chemistry and Material Science, College of Science, Nanjing Forestry University, Nanjing, Jiangsu 210037, China;* orcid.org/0000-0002-8641-2430

Shuaishuai Zhu − *School of Materials Science and Engineering, Nanjing Institute of Technology, Nanjing, Jiangsu 211167, China*

Tong Li − *Department of Biomedical Engineering, College of Engineering and Applied Sciences, Nanjing National Laboratory of Microstructures, Jiangsu Key Laboratory of Artificial Functional Materials, Nanjing University, Nanjing, Jiangsu 210023, China*

Complete contact information is available at: https://pubs.acs.org/10.1021/acs.nanolett.3c04548

Notes

The authors declare no competing financial interest.

■ ACKNOWLEDGMENTS

This work was supported by the National Natural Science Foundation of China (22374071), the National Key R&D Program of China (2019YFA0709200 and 2021YFF1200700), the PAPD Program, State Key Laboratory of Analytical Chemistry for Life Science (5431ZZXM2306), and Fundamental Research Funds for the Central Universities (202200325 and 021314380228).

■ REFERENCES

(1) Majowicz, S. E.; Musto, J.; Scallan, E.; Angulo, F. J.; Kirk, M.; O'Brien, S. J.; Jones, T. F.; Fazil, A.; Hoekstra, R. M. International Collaboration on Enteric Disease 'Burden of Illness, S., The global burden of nontyphoidal *Salmonella* gastroenteritis. *Clin. Infect. Dis.* **2010**, *50* (6), 882−889.

(2) Cash-Goldwasser, S.; Barry, M. CDC Yellow Book 2018: Health Information for International Travel. *Clin. Infect. Dis.* **2018**, *66* (7), 1157−1158.

(3) Byndloss, M. X.; Baumler, A. J. The germ-organ theory of non-communicable diseases. *Nat. Rev. Microbiol.* **2018**, *16* (2), 103−110.

(4) Gareau, M. G.; Sherman, P. M.; Walker, W. A. Probiotics and the gut microbiota in intestinal health and disease. *Nat. Rev. Gastro. Hepat.* **2010**, *7* (9), 503−514.

(5) Baumler, A. J.; Sperandio, V. Interactions between the microbiota and pathogenic bacteria in the gut. *Nature* **2016**, *535* (7610), 85−93.

(6) Litvak, Y.; Mon, K. K. Z.; Nguyen, H.; Chanthavixay, G.; Liou, M.; Velazquez, E. M.; Kutter, L.; Alcantara, M. A.; Byndloss, M. X.; Tiffany, C. R.; Walker, G. T.; Faber, F.; Zhu, Y.; Bronner, D. N.; Byndloss, A. J.; Tsolis, R. M.; Zhou, H.; Baumler, A. J. Commensal *Enterobacteriaceae* Protect against *Salmonella* Colonization through Oxygen Competition. *Cell Host Microbe* **2019**, *25* (1), 128−139.

(7) Lu, Z.; Imlay, J. A. When anaerobes encounter oxygen: mechanisms of oxygen toxicity, tolerance and defence. *Nat. Rev. Microbiol.* **2021**, *19* (12), 774−785.

(8) Rogers, A. P.; Mileto, S. J.; Lyras, D. Impact of enteric bacterial infections at and beyond the epithelial barrier. *Nat. Rev. Microbiol.* **2023**, *21* (4), 260−274.

(9) Turner, J. R. Intestinal mucosal barrier function in health and disease. *Nat. Rev. Immunol.* **2009**, *9* (11), 799−809.

(10) Tilg, H.; Adolph, T. E.; Trauner, M. Gut-liver axis: Pathophysiological concepts and clinical implications. *Cell Metab.* **2022**, *34* (11), 1700−1718.
(11) Li, J.; Cha, R.; Zhao, X.; Guo, H.; Luo, H.; Wang, M.; Zhou, F.; Jiang, X. Gold Nanoparticles Cure Bacterial Infection with Benefit to Intestinal Microflora. *ACS Nano* **2019**, *13* (5), 5002−5014.
(12) Zhou, J.; Li, M.; Chen, Q.; Li, X.; Chen, L.; Dong, Z.; Zhu, W.; Yang, Y.; Liu, Z.; Chen, Q. Programmable probiotics modulate inflammation and gut microbiota for inflammatory bowel disease treatment after effective oral delivery. *Nat. Commun.* **2022**, *13* (1), 3432.
(13) Cao, F.; Jin, L.; Gao, Y.; Ding, Y.; Wen, H.; Qian, Z.; Zhang, C.; Hong, L.; Yang, H.; Zhang, J.; Tong, Z.; Wang, W.; Chen, X.; Mao, Z. Artificial-enzymes-armed *Bifidobacterium longum* probiotics for alleviating intestinal inflammation and microbiota dysbiosis. *Nat. Nanotechnol.* **2023**, *18* (6), 617−627.
(14) Piewngam, P.; Zheng, Y.; Nguyen, T. H.; Dickey, S. W.; Joo, H. S.; Villaruz, A. E.; Glose, K. A.; Fisher, E. L.; Hunt, R. L.; Li, B.; Chiou, J.; Pharkjaksu, S.; Khongthong, S.; Cheung, G. Y. C.; Kiratisin, P.; Otto, M. Pathogen elimination by probiotic *Bacillus* via signalling interference. *Nature* **2018**, *562* (7728), 532−537.
(15) Song, Q.; Zheng, C.; Jia, J.; Zhao, H.; Feng, Q.; Zhang, H.; Wang, L.; Zhang, Z.; Zhang, Y. A Probiotic Spore-Based Oral Autonomous Nanoparticles Generator for Cancer Therapy. *Adv. Mater.* **2019**, *31* (43), 1903793.
(16) Chen, Q.-W.; Qiao, J.-Y.; Cao, M.-W.; Han, Z.-Y.; Zeng, X.; Zhang, X.-Z. Spore germinator-loaded polysaccharide microspheres ameliorate colonic inflammation and tumorigenesis through remodeling gut microenvironment. *Mater. Today* **2023**, *63*, 32−49.
(17) Mutlu, A.; Trauth, S.; Ziesack, M.; Nagler, K.; Bergeest, J. P.; Rohr, K.; Becker, N.; Hofer, T.; Bischofs, I. B. Phenotypic memory in *Bacillus subtilis* links dormancy entry and exit by a spore quantity-quality tradeoff. *Nat. Commun.* **2018**, *9* (1), 69.
(18) Cao, J.; Yu, Z.; Liu, W.; Zhao, J.; Zhang, H.; Zhai, Q.; Chen, W. Probiotic characteristics of *Bacillus coagulans* and associated implications for human health and diseases. *J. Funct. Foods* **2020**, *64*, 103643−103654.
(19) Wei, H.; Wang, E. Nanomaterials with enzyme-like characteristics (nanozymes): next-generation artificial enzymes. *Chem. Soc. Rev.* **2013**, *42* (14), 6060−6093.
(20) Liang, M.; Yan, X. Nanozymes: From New Concepts, Mechanisms, and Standards to Applications. *Acc. Chem. Res.* **2019**, *52* (8), 2190−2200.
(21) Xu, Y.; Luo, Y.; Weng, Z.; Xu, H.; Zhang, W.; Li, Q.; Liu, H.; Liu, L.; Wang, Y.; Liu, X.; Liao, L.; Wang, X. Microenvironment-Responsive Metal-Phenolic Nanozyme Release Platform with Antibacterial, ROS Scavenging, and Osteogenesis for Periodontitis. *ACS Nano* **2023**, *17*, 18732.
(22) Zhang, W.; Hu, S.; Yin, J. J.; He, W.; Lu, W.; Ma, M.; Gu, N.; Zhang, Y. Prussian Blue Nanoparticles as Multienzyme Mimetics and Reactive Oxygen Species Scavengers. *J. Am. Chem. Soc.* **2016**, *138* (18), 5860−5865.
(23) Samuel, E. L.; Marcano, D. C.; Berka, V.; Bitner, B. R.; Wu, G.; Potter, A.; Fabian, R. H.; Pautler, R. G.; Kent, T. A.; Tsai, A. L.; Tour, J. M. Highly efficient conversion of superoxide to oxygen using hydrophilic carbon clusters. *Proc. Natl. Acad. Sci. U.S.A.* **2015**, *112* (8), 2343−2348.
(24) Zhang, R.; Yan, X.; Fan, K. Nanozymes Inspired by Natural Enzymes. *Acc. Mater. Res.* **2021**, *2* (7), 534−547.
(25) Huang, Y.; Ren, J.; Qu, X. Nanozymes: Classification, Catalytic Mechanisms, Activity Regulation, and Applications. *Chem. Rev.* **2019**, *119* (6), 4357−4412.
(26) Zhao, S.; Li, Y.; Liu, Q.; Li, S.; Cheng, Y.; Cheng, C.; Sun, Z.; Du, Y.; Butch, C. J.; Wei, H. An Orally Administered CeO_2@ Montmorillonite Nanozyme Targets Inflammation for Inflammatory Bowel Disease Therapy. *Adv. Funct. Mater.* **2020**, *30* (45), 2004692.
(27) Liu, C.; Gui, L.; Zheng, J.-J.; Xu, Y.-Q.; Song, B.; Yi, L.; Jia, Y.; Taledaohan, A.; Wang, Y.; Gao, X.; Qiao, Z.-Y.; Wang, H.; Tang, Z. Intrinsic Strain-Mediated Ultrathin Ceria Nanoantioxidant. *J. Am. Chem. Soc.* **2023**, *145*, 19086.
(28) Kim, Y. G.; Lee, Y.; Lee, N.; Soh, M.; Kim, D.; Hyeon, T. Ceria-Based Therapeutic Antioxidants for Biomedical Applications. *Adv. Mater.* **2023**, 2210819.
(29) Chen, J.; Patil, S.; Seal, S.; McGinnis, J. F. Rare earth nanoparticles prevent retinal degeneration induced by intracellular peroxides. *Nat. Nanotechnol.* **2006**, *1* (2), 142−150.
(30) Oishi, M.; Yoshikawa, H.; Sueoka, N. Synchronous and Dichotomous Replications of the *Bacillus subtilis* Chromosome During Spore Germination. *Nature* **1964**, *204* (4963), 1069−1073.
(31) Liu, T.; Xiao, B.; Xiang, F.; Tan, J.; Chen, Z.; Zhang, X.; Wu, C.; Mao, Z.; Luo, G.; Chen, X.; Deng, J. Ultrasmall copper-based nanoparticles for reactive oxygen species scavenging and alleviation of inflammation related diseases. *Nat. Commun.* **2020**, *11* (1), 2788.
(32) Liu, C.; Cai, Y.; Wang, J.; Liu, X.; Ren, H.; Yan, L.; Zhang, Y.; Yang, S.; Guo, J.; Liu, A. Facile Preparation of Homogeneous Copper Nanoclusters Exhibiting Excellent Tetraenzyme Mimetic Activities for Colorimetric Glutathione Sensing and Fluorimetric Ascorbic Acid Sensing. *ACS Appl. Mater. Interfaces* **2020**, *12* (38), 42521−42530.
(33) Zhang, F.; Wang, B.; Liu, S.; Chen, Y.; Lin, Y.; Liu, Z.; Zhang, X.; Yu, B. *Bacillus subtilis* revives conventional antibiotics against *Staphylococcus aureus* osteomyelitis. *Microb. Cell Fact.* **2021**, *20* (1), 102−117.
(34) Wei, G.; Liu, Q.; Wang, X.; Zhou, Z.; Zhao, X.; Zhou, W.; Liu, W.; Zhang, Y.; Liu, S.; Zhu, C.; Wei, H. A probiotic nanozyme hydrogel regulates vaginal microenvironment for *Candida* vaginitis therapy. *Sci. Adv.* **2023**, *9* (20), eadg0949.
(35) Qiao, Z.; Zhang, K.; Liu, J.; Cheng, D.; Yu, B.; Zhao, N.; Xu, F. J. Biomimetic electrodynamic nanoparticles comprising ginger-derived extracellular vesicles for synergistic anti-infective therapy. *Nat. Commun.* **2022**, *13* (1), 7164.
(36) Nathan, C.; Cunningham-Bussel, A. Beyond oxidative stress: an immunologist's guide to reactive oxygen species. *Nat. Rev. Immunol.* **2013**, *13* (5), 349−361.
(37) Xiao, Y.; Lu, C.; Liu, Y.; Kong, L.; Bai, H.; Mu, H.; Li, Z.; Geng, H.; Duan, J. Encapsulation of *Lactobacillus rhamnosus* in Hyaluronic Acid-Based Hydrogel for Pathogen-Targeted Delivery to Ameliorate Enteritis. *ACS Appl. Mater. Interfaces* **2020**, *12* (33), 36967−36977.
(38) Cook, M. T.; Tzortzis, G.; Charalampopoulos, D.; Khutoryanskiy, V. V. Microencapsulation of probiotics for gastrointestinal delivery. *J. Controlled Release* **2012**, *162* (1), 56−67.
(39) Liu, J.; Wang, Y.; Heelan, W. J.; Chen, Y.; Li, Z.; Hu, Q. Mucoadhesive probiotic backpacks with ROS nanoscavengers enhance the bacteriotherapy for inflammatory bowel diseases. *Sci. Adv.* **2022**, *8* (45), eabp8798.
(40) Mu, H.; Bai, H.; Sun, F.; Liu, Y.; Lu, C.; Qiu, Y.; Chen, P.; Yang, Y.; Kong, L.; Duan, J. Pathogen-targeting glycovesicles as a therapy for salmonellosis. *Nat. Commun.* **2019**, *10* (1), 4039.
(41) Liu, H.; Cai, Z.; Wang, F.; Hong, L.; Deng, L.; Zhong, J.; Wang, Z.; Cui, W. Colon-Targeted Adhesive Hydrogel Microsphere for Regulation of Gut Immunity and Flora. *Adv. Sci.* **2021**, *8* (18), 2101619.
(42) Schirmer, M.; Garner, A.; Vlamakis, H.; Xavier, R. J. Microbial genes and pathways in inflammatory bowel disease. *Nat. Rev. Microbiol.* **2019**, *17* (8), 497−511.
(43) Ouyang, J.; Deng, B.; Zou, B.; Li, Y.; Bu, Q.; Tian, Y.; Chen, M.; Chen, W.; Kong, N.; Chen, T.; Tao, W. Oral Hydrogel Microbeads-Mediated In Situ Synthesis of Selenoproteins for Regulating Intestinal Immunity and Microbiota. *J. Am. Chem. Soc.* **2023**, *145* (22), 12193−12205.
(44) Natividad, J. M.; Lamas, B.; Pham, H. P.; Michel, M. L.; Rainteau, D.; Bridonneau, C.; da Costa, G.; van Hylckama Vlieg, J.; Sovran, B.; Chamignon, C.; Planchais, J.; Richard, M. L.; Langella, P.; Veiga, P.; Sokol, H. *Bilophila* wadsworthia aggravates high fat diet induced metabolic dysfunctions in mice. *Nat. Commun.* **2018**, *9* (1), 2802.

https://doi.org/10.1021/acs.nanolett.3c04548
Nano Lett. 2024, 24, 2289−2298

(45) Bernard, D.; Verschraegen, G.; Claeys, G.; Lauwers, S.; Rosseel, P. *Bilophila* wadsworthia Bacteremia in a Patient with Gangrenous Appendicitis. *Clin. Infect. Dis.* **1994**, *18* (6), 1023−1024.
(46) Konikoff, T.; Gophna, U. *Oscillospira*: a Central, Enigmatic Component of the Human Gut Microbiota. *Trends Microbiol.* **2016**, *24* (7), 523−524.
(47) Hosomi, K.; Saito, M.; Park, J.; Murakami, H.; Shibata, N.; Ando, M.; Nagatake, T.; Konishi, K.; Ohno, H.; Tanisawa, K.; Mohsen, A.; Chen, Y. A.; Kawashima, H.; Natsume-Kitatani, Y.; Oka, Y.; Shimizu, H.; Furuta, M.; Tojima, Y.; Sawane, K.; Saika, A.; Kondo, S.; Yonejima, Y.; Takeyama, H.; Matsutani, A.; Mizuguchi, K.; Miyachi, M.; Kunisawa, J. Oral administration of *Blautia wexlerae* ameliorates obesity and type 2 diabetes via metabolic remodeling of the gut microbiota. *Nat. Commun.* **2022**, *13* (1), 4477.

https://doi.org/10.1021/acs.nanolett.3c04548
Nano Lett. 2024, 24, 2289−2298